JBIC Journal of Biological Inorganic Chemistry
https://doi.org/10.1007/s00775-021-01905-4

ORIGINAL PAPER

Selected polyoxopalladates as promising and selective antitumor drug candidates

Andjelka M. Isakovic[1] · Mirjana B. Čolović[2] · Tian Ma[3] · Xiang Ma[3] · Marija Jeremic[1] · Marko Gerić[4] · Goran Gajski[4] · Sonja Misirlic-Dencic[1] · Ulrich Kortz[3] · Danijela Krstić[5]

Received: 8 June 2021 / Accepted: 10 September 2021

Abstract

Polyoxo-noble-metalates (PONMs), a class of molecular noble metal-oxo nanoclusters that combine features of both polyoxometalates and noble metals, are a promising platform for the development of next-generation antitumor metallodrugs. This study aimed to evaluate the antitumor potential against human neuroblastoma cells (SH-SY5Y), as well as toxicity towards healthy human peripheral blood cells (HPBCs), of five polyoxopalladates(II): ($Na_8[Pd_{13}As_8O_{34}(OH)_6]\cdot 42H_2O$ (**Pd_{13}**), $Na_4[SrPd_{12}O_6(OH)_3(PhAsO_3)_6(OAc)_3]\cdot 2NaOAc\cdot 32H_2O$ (**$SrPd_{12}$**), $Na_6[Pd_{13}(AsPh)_8O_{32}]\cdot 23H_2O$ (**$Pd_{13}L$**), $Na_{12}[SnO_8Pd_{12}(PO_4)_8]\cdot 43H_2O$ (**$SnPd_{12}$**), and $Na_{12}[PbO_8Pd_{12}(PO_4)_8]\cdot 38H_2O$ (**$PbPd_{12}$**)), as the largest subset of PONMs. A pure inorganic, **Pd_{13}**, was found as the most potent and selective antineuroblastoma agent with IC_{50} values (μM) of 7.2 ± 2.2 and 4.4 ± 1.2 for 24 and 48 h treatment, respectively, even lower than cisplatin (28.4 ± 7.4 and 11.6 ± 0.8). The obtained IC_{50} values (μM) for 24/48 h treatment with **$SrPd_{12}$** and **$Pd_{13}L$** were $75.8 \pm 6.7/76.7 \pm 22.9$ and $63.8 \pm 3.6/21.4 \pm 10.8$, respectively, whereas **$SnPd_{12}$** and **$PbPd_{12}$** did not remarkably affect the SH-SY5Y viability ($IC_{50} >> 100$ μM). **Pd_{13}** caused depolarisation of inner mitochondrial membrane prior to superoxide ion hyperproduction, followed by caspase activation, DNA fragmentation and cell cycle arrest, all hallmarks of apoptotic cell death, and accompanied by an increase in acidic vesicles content, suggestive of autophagy induction. Importantly, **Pd_{13}** demonstrated the antitumor effect at concentrations not cytogenotoxic for normal HPBCs. On the contrary, **$SrPd_{12}$** and **$Pd_{13}L$** at concentrations $\geq 1/3$ IC_{50} (24 h) decreased HPBC viability and increased % tail DNA up to 42% and 3.05 times, respectively, related to control. **$SnPd_{12}$** and **$PbPd_{12}$**, previously confirmed promising antileukemic agents, did not exhibit cytogenotoxicity to HPBCs, and thus could be regarded as tumor cell specific and selective drug candidates.

✉ Sonja Misirlic-Dencic
sonja.misirlic-dencic@med.bg.ac.rs

✉ Ulrich Kortz
u.kortz@jacobs-university.de

✉ Danijela Krstić
danijela.krstic@med.bg.ac.rs

[1] Institute of Medical and Clinical Biochemistry, Faculty of Medicine, University of Belgrade, Belgrade, Serbia

[2] Department of Physical Chemistry, "Vinča" Institute of Nuclear Sciences-National Institute of the Republic of Serbia, University of Belgrade, Belgrade, Serbia

[3] Department of Life Sciences and Chemistry, Jacobs University, Bremen, Germany

[4] Institute for Medical Research and Occupational Health, Mutagenesis Unit, Zagreb, Croatia

[5] Institute of Medical Chemistry, Faculty of Medicine, University of Belgrade, Belgrade, Serbia

Published online: 21 September 2021

Graphic abstract

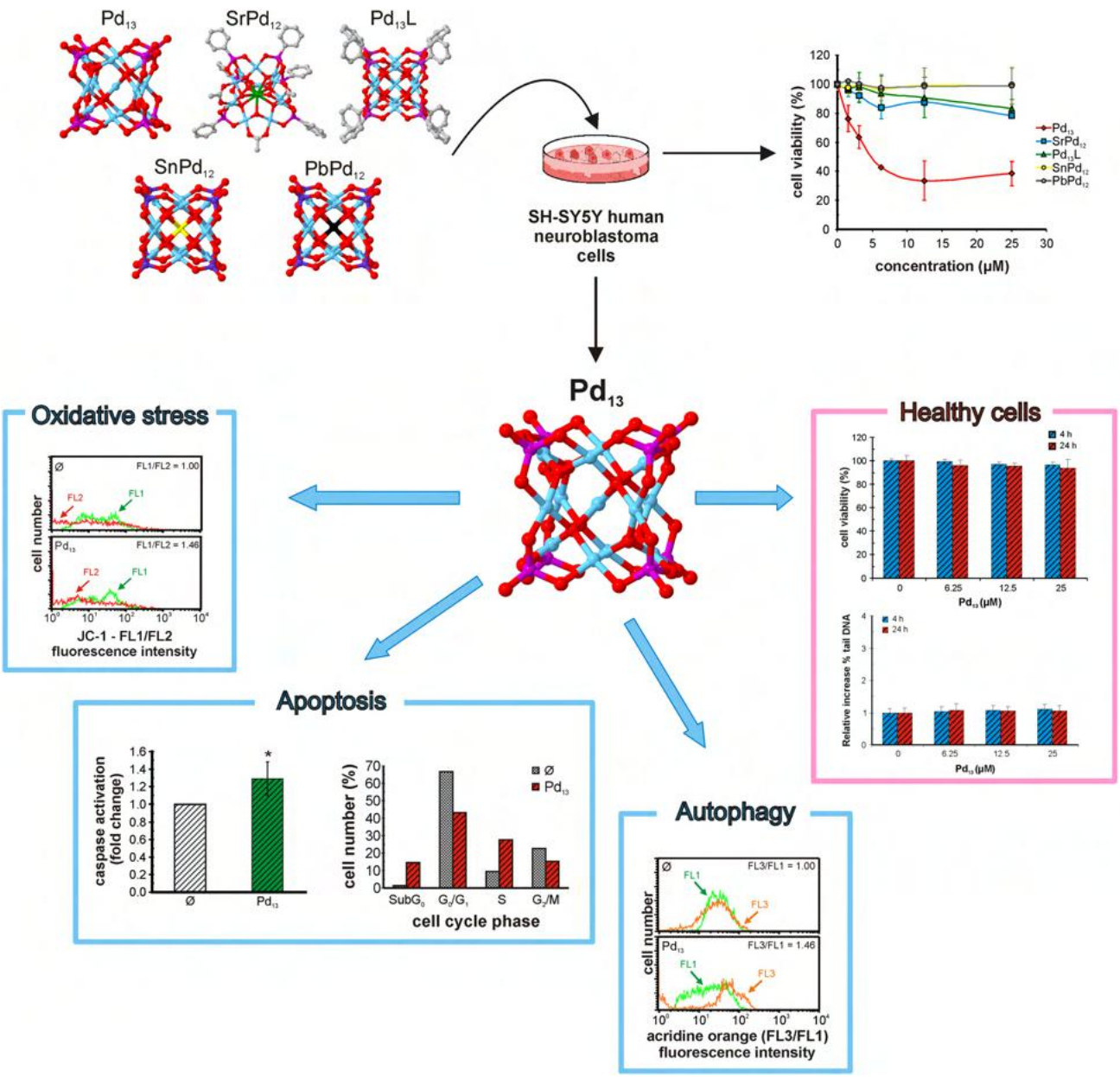

Keywords Human neuroblastoma cells (SH-SY5Y) · Polyoxopalladates · Antitumor · Cytogenotoxicity · Human peripheral blood cells

Abbreviations

AO	Acridine orange
CDDP	Cisplatin
EB	Ethidium bromide
HPBC	Human peripheral blood cell
PBMC	Peripheral blood mononuclear cell
PBS	Phosphate-buffered saline
PI	Propidium iodide
POM	Polyoxometalate
PONM	Polyoxo-noble-metalate
POP	Polyoxopalladate

Introduction

The application of metal-based compounds in cancer therapy started in the 1970s when "cisplatin" [$Pt(NH_3)_2Cl_2$] was approved for clinical use in treating metastatic testicular and ovarian cancers [1]. Nowadays, platinum-based drugs such as cisplatin, carboplatin, oxaliplatin, nedaplatin, heptaplatin, and lobaplatin belong to the most frequently prescribed chemotherapeutics [2–7]. Nevertheless, their application results in toxic side effects toward normal tissues such as neuro-, hepato- and nephrotoxicity [8–10] and in intrinsic and/or acquired tumor resistance [11], which are considered as major limiting factors in the clinical use of platinum antitumor agents [12, 13]. To overcome these limitations, the development of novel antitumor agents has been directed to other noble metals [14], including palladium(II) which is a d^8 metal ion and the lighter congener of platinum(II). The first palladium complexes exhibiting high activities were synthesized in the 1980s [15–17], and > 1000 palladium compounds, some with even more potent antitumor potential than cisplatin, have been synthesized and tested against a variety of tumor cells in vitro and in vivo [3, 18–23].

Polyoxometalates (POMs) are another class of metal-based compounds reported to exhibit promising in vitro and in vivo cytotoxic action against various types of malignant cells in the last 3 decades. POMs are discrete, negatively charged metal-oxo clusters containing early *d*-block metal ions in high oxidation states surrounded by oxo ligands. The literature on promising POM-based antitumor agents is mostly based on classical POMs such as polyoxotungstates, -molybdates, and -vanadates [24–30]. Besides, polyoxo-noble-metalates (PONMs) are an emerging class of molecular noble metal-oxo nanoclusters combining features of both POMs and noble metals, and present a promising platform for the development of next-generation antitumor metallodrugs [31]. Thus, it is of prime interest to evaluate the antitumor potential of polyoxopalladates(II) (POPs), which are discrete, anionic palladium-oxo clusters with different shapes, sizes and compositions [32]. Although the first POP was synthesized in 2008 [33] and nowadays, these POMs represent the largest continuously growing subclass of PONMs, relevant studies on their biological activities are rare despite the abundant presence of palladium (Pd), a constituent of established antitumor drug candidates [23].

Based on the above information, in this study, the antitumor properties of the following five POP salts (Fig. 1) differing in shape, charge, size, and composition:

(1) Arsenate-capped nanocube $Na_8[Pd_{13}As_8O_{34}(OH)_6]\cdot 42H_2O$—**$Pd_{13}$** [33],

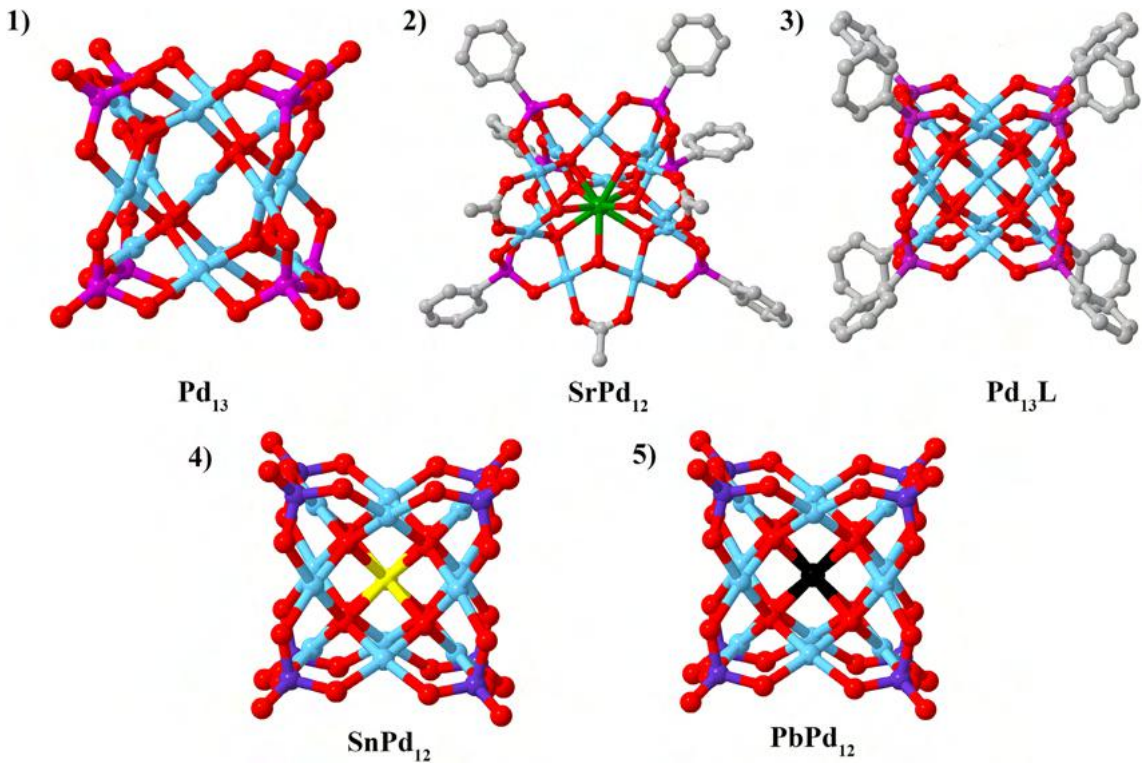

Fig. 1 Ball-and-stick representation of the POPs used in this study: **Pd_{13}** (1), **$SrPd_{12}$** (2), **$Pd_{13}L$** (3), **$SnPd_{12}$** (4), **$PbPd_{12}$** (5). Color codes: light blue, Pd; yellow, Sn; black, Pb; green, Sr; purple, As; violet, P; grey, C and red, O. Hydrogen atoms are omitted to simplify structures

(2) Phenylarsonate-capped open-shell structure $Na_4[SrPd_{12}O_6(OH)_3(PhAsO_3)_6(OAc)_3]\cdot 2NaOAc\cdot 32H_2O$—**SrPd$_{12}$** [34],
(3) Phenylarsonate-capped nanocube $Na_6[Pd_{13}O_8(PhAsO_3)_8]\cdot 23H_2O$—**Pd$_{13}$L** [35],
(4) Phosphate-capped nanocube $Na_{12}[Sn^{IV}O_8Pd_{12}(PO_4)_8]\cdot 43H_2O$—**SnPd$_{12}$** [36], and
(5) Phosphate-capped nanocube $Na_{12}[Pb^{IV}O_8Pd_{12}(PO_4)_8]\cdot 38H_2O$—**PbPd$_{12}$** [36]

were evaluated in vitro using the human neuroblastoma cell line (SH-SY5Y) as a model system. Neuroblastoma cells are a useful and cost-effective model that has been widely used to study pharmacological activities of potential antitumor agents. Neuroblastoma is the most common childhood malignance of the nervous system, and amongst the most challenging to be treated due to the extreme aggressiveness and resistance, and thus deserves a special interest regarding research of novel potential chemotherapeutics [37, 38]. Since the priority in the investigation of novel potential drugs is the assessment of their safety, the cytogenotoxicity of the selected POPs towards normal non-target cells was evaluated as well. For this purpose, evaluation of cell viability and the comet assay were employed on human peripheral blood cells (HPBCs).

This work investigates the molecular mechanism of the POP-induced antitumor action using flow cytometric analysis of oxidative stress, caspase activation, cell cycle distribution, and autophagy presence. Moreover, the present study is a continuation of the previous work in which antileukemic action of two nanocubic POPs containing tetravalent metal ions (Sn^{IV} and Pb^{IV}) incorporated inside the Pd_{12} host, **SnPd$_{12}$** and **PbPd$_{12}$**, towards human acute promyelocytic cell line HL-60 was confirmed [36]. The satisfactory antineuroblastoma action of three investigated POPs (**Pd$_{13}$**, **SrPd$_{12}$**, and **Pd$_{13}$L**), highlighting **Pd$_{13}$** as the most promising drug candidate, was demonstrated. Furthermore, no cytogenotoxicity towards normal cells was observed for **Pd$_{13}$** as well as for potential antileukemic drugs, **SnPd$_{12}$** and **PbPd$_{12}$**. These findings indicate that POPs could be considered as prospective candidates in the development of selective, tumor specific and tunable at molecular level next-generation Pd-based chemotherapeutics.

Experimental section

Syntheses

All POPs investigated in this study were prepared according to previously published procedures. $Na_8[Pd_{13}As_8O_{34}(OH)_6]\cdot 42H_2O$ (**Pd$_{13}$**), $[SrPd_{12}O_6(OH)_3(PhAsO_3)_6(OAc)_3]\cdot 2NaOAc\cdot 32H_2O$ (**SrPd$_{12}$**), $Na_6[Pd_{13}O_8(PhAsO_3)_8]\cdot 23H_2O$ (**Pd$_{13}$L**) were synthesized according to references [33, 34], and [35], respectively. $Na_{12}[Sn^{IV}O_8Pd_{12}(PO_4)_8]\cdot 43H_2O$ (**SnPd$_{12}$**) and $Na_{12}[Pb^{IV}O_8Pd_{12}(PO_4)_8]\cdot 38H_2O$ (**PbPd$_{12}$**) were prepared according to reference [36].

Preparation of POP solutions

Stock aqueous solutions (5 mM) of **Pd$_{13}$**, **SrPd$_{12}$**, and **Pd$_{13}$L** were prepared by vigorous mixing at 65 °C for 4 h, whereas **SnPd$_{12}$** and **PbPd$_{12}$** were dissolved at 80 °C for 8 h for preparing aqueous stock solutions of 500 µM. For the antitumor assessment, working solutions used were prepared by diluting the stock solutions in a complete F12/MEM medium up to desired final concentrations. Cisplatin (CDDP, Sigma-Aldrich, St. Louis, MO, USA) was dissolved in water for stock solution of 3 mM, while working solutions were prepared by dilution in cell culture medium. For the normal cell toxicity assessment, working solutions were prepared by diluting the stock solutions with phosphate-buffered saline (PBS) up to desired concentrations. 10 µL of the stock/working solutions of **Pd$_{13}$**, **SrPd$_{12}$**, and **Pd$_{13}$L** were added to 990 µL whole blood samples yielding final concentrations (Figs. 7 and 8), whereas final concentrations of **SnPd$_{12}$** and **PbPd$_{12}$** (Figs. 7 and 8) were prepared by adding 100 µL of the stock/working solutions to 900 µL whole blood samples.

Antitumor assessment

Cell line

Antitumor assessment was conducted on the SH-SY5Y commercial human neuroblastoma cell line, obtained from the European Collection of Animal Cell Cultures (Salisbury, UK). The cells were cultured at 37 °C in a humidified atmosphere with 5% CO_2, in F12/MEM medium, supplemented with 1% glutamine (2 mM), 1% antibiotic/antimycotic mixture, and 10% fetal bovine serum (all from PAA, Pasching, Austria).

Cell viability

Cells were cultured in flat bottom 96-well plates (1×10^4 and 0.6×10^4 cells per well for 24 and 48 h, respectively). The number of viable cells after the treatment was assessed using an acid phosphatase viability assay. The number of viable cells is considered to be proportional to the activity of endogenous lysosomal acid phosphatase. Acid phosphatase catalyzes the hydrolysis of *p*-nitrophenyl phosphate to *p*-nitrophenol. Deprotonation of *p*-nitrophenol in the alkaline medium then results in the formation of the yellow-colored *p*-nitrophenolate. The intensity of the color is proportional to the activity of acid phosphatase (i.e. the number

of living cells) and is determined spectrophotometrically by measuring the absorbance at an automated plate reader (Tecan, Dorset, UK) at 405 nm. The assay was performed exactly as previously described [39]. Results were analyzed using GraphPad Prism 4.0. One-way ANOVA with Dunnett's Multiple Comparison Test was used to determine statistically significant differences between untreated cells and cells treated with different concentrations of POPs. Non-linear regression curve fitting was used to calculate IC_{50} values (the concentration that decreases the cell viability to 50%). Detailed information regarding curve fitting is available in supplementary material. Two-way ANOVA followed by Bonferroni posttest was used for IC_{50} values comparison. A p value of <0.05 was considered statistically significant.

Investigation of antitumor mechanism of action

In the experiments investigating the molecular mechanisms of POPs' toxicity towards SH-SY5Y cells, the IC_{50} concentrations of $\mathbf{Pd_{13}}$, $\mathbf{SrPd_{12}}$ and $\mathbf{Pd_{13}L}$ were used. The cells were cultured in 12-well plates (10×10^5 cells per well), and after the treatment stained with appropriate fluorochromes and analyzed on FACSCalibur flow cytometer with the CellQuest Pro software (BD Biosciences, Heidelberg, Germany). The cells were stained exactly as instructed by manufacturer for 25 min at 37 °C, washed in PBS (except after propidium iodide (PI) staining), and then analyzed. Each analysis included 10,000 analyzed events (cells). Statistical analysis was done using GraphPad Prism 4.0 by t test.

Oxidative stress and mitochondrial membrane potential

The level of superoxide ion, produced after 2 and 4 h of treatment, was determined using dihydroethidium (DHE, 20 μM; Sigma-Aldrich, St. Louis, MO, USA). In the presence of superoxide ion, DHE is oxidized to 2-hydroxyethidium emitting red fluorescence whose intensity is detected by flow cytometry (FL2 channel). The results are presented as fold change in median fluorescence intensity in treated cells compared to untreated (control) cells in which the fluorescence is arbitrarily set to 1.0 [39].

The mitochondrial membrane potential was assessed using JC-1 (Thermo Fisher Scientific, Waltham, MA, USA), a lipophilic cation that aggregates upon membrane polarization yielding a red fluorescence. Upon an increase in mitochondrial membrane potential (depolarization) JC-1 stays or reverts to its monomeric, green-fluorescing form, and is thus used as a marker of mitochondrial membrane potential. The results are expressed as a fold change in green/red median fluorescence ratio (FL1/FL2) compared to control, untreated, neuroblastoma cells (FL1/FL2 is arbitrarily set to 1.0). An increased FL1/FL2 ratio indicates mitochondrial depolarization [39].

Caspase activation and cell cycle distribution

FITC-conjugated pancaspase inhibitor ApoStat (R&D Systems, Minneapolis, MN, USA) which yields green fluorescence (FL1), was used to determine pancaspase activity after 24 h treatment. The results are presented as a fold change in median green fluorescence intensity (FL1) in treated neuroblastoma cells compared to untreated, control cells in which the fluorescence intensity was arbitrarily set to 1.0 [40].

The cell cycle was examined by staining ethanol-fixed treated (24 h) and untreated neuroblastoma cells with PI. Upon RNA degradation, PI binds to the DNA in a 1:1 ratio and emits red fluorescence (FL2). The mean fluorescence intensity thus corresponds to the DNA content in the appropriate phase of the cell cycle (G_0/G_1, S, G_2/M). The cells with hypodiploid DNA content ($SubG_0$) have fragmented DNA and are considered apoptotic. The results are presented as percentage of cells in different phases of the cell cycle [41].

Acidic intracellular vesicles content

Acidic vesicles content in 24 h treated neuroblastoma cells was assessed by pH-sensitive supravital dye acridine orange (AO), (R&D Systems, Minneapolis, MN, USA). AO is a green fluorophore (FL1) that aggregates in acidic vesicles yielding orange fluorescence (FL3). Therefore, the increase in acidic vesicles content, indicative for autophagy induction, was determined calculating the fold change in median green/orange fluorescence ratio (FL3/FL1) of treated neuroblastoma cells compared to FL3/FL1 set to 1.00 for the untreated, control, neuroblastoma cells [39].

Normal cell toxicity

Blood sampling and treatment

The effect of POPs was evaluated in human peripheral blood cells (HPBCs) obtained from a young, healthy, non-smoking female donor (25 years old). The subject gave informed consent to participate in this study, which was approved by the Institutional Ethics Committee and observed the ethical principles of the Declaration of Helsinki. According to the questionnaire, which the donor completed, she had not been exposed to ionizing radiation or genotoxic chemicals that might have interfered with the results of the testing for a year before blood sampling. The blood was drawn by antecubital venipuncture into vacutainers (Becton Dickinson, Franklin Lakes, USA) containing lithium heparin as anticoagulant.

To obtain the final concentrations, the aliquots of POP solutions were added to the whole blood samples which then were incubated at 37 °C for 4 and 24 h.

Cell viability (cytotoxicity) assay

The cytotoxicity of POPs in peripheral blood mononuclear cells (PBMCs) was determined by differential staining with AO and ethidium bromide (EB) and by fluorescence microscopy [42]. Whole blood samples were treated with three different concentrations, including 12.5 and 25 µM of all five investigated POPs, selected from those used in acid phosphatase assay, so that at least one of them approximately corresponds to 24 h - IC_{50} value obtained on SH-SY5Y or HL-60 cells [36]. After treatment, the PBMCs were isolated by the histopaque density gradient centrifugation method. The slides were prepared using 200 µLof PBMCs and 2 µL of stain (AO and EB, both diluted in PBS). A total of 100 cells per repetition were examined with an epifluorescence microscope (Olympus BX51, Tokyo, Japan). The cells were divided in two categories: live cells with a functional membrane and with uniform green staining of the nucleus and dead cells with uniform red staining of the nucleus. The difference in the cell viability between control and exposed samples was done by the Student *t* test. Data were considered statistically significant at $p < 0.05$.

Alkaline comet (SCGE) assay

The alkaline comet assay was essentially carried out as described by Singh et al. [43] with only minor modifications [44] following recommendations for describing comet assay procedures and results [45]. After the exposure to different concentrations (µM) of POPs for 4 and 24 h, 5 µL of whole blood was embedded in 100 µL of 0.5% low melting point agarose matrix and subsequently lysed (2.5 M NaCl, 100 mM $EDTANa_2$, 10 mM Tris, 1% sodium sarcosinate, 1% Triton X-100, 10% DMSO, pH 10) overnight at 4 °C. After the lysis, the slides were placed into an alkaline solution (300 mM NaOH, 1 mM $EDTANa_2$, pH 13) for 20 min at 4 °C to allow DNA unwinding and subsequently electrophoresed for 20 min at 1 V/cm. Finally, the slides were neutralized in 0.4 M Tris buffer (pH 7.5) for 5 min three times, stained with EB (10 µg/mL) and analyzed at 250 × magnification using the Orthoplan epifluorescence microscope (Leitz, Wetzlar, Germany) connected through a camera to an image analysis system (Comet Assay II; Perceptive Instruments Ltd., Haverhill, Suffolk, UK). One hundred randomly captured comets from each slide were examined. The percent of tail DNA was used to measure the degree of DNA damage. The comet assay results were evaluated using the Statistica13.2 program package (Dell Inc., USA). To normalize the distribution and equalize the variances of the comet assay data, a logarithmic transformation was applied. Multiple comparisons between groups were done by means of ANOVA on log-transformed data. Post hoc analyses of the differences were done by the Scheffé test. Data were considered statistically significant at $p < 0.05$.

Results and discussion

POPs influence on viability of human neuroblastoma cells

The viability of human neuroblastoma cell line (SH-SY5Y) was examined using the acid phosphatase assay after 24 and 48 h treatment with investigated POPs (Fig. 2).

The obtained results suggest that after 24 h treatment **Pd_{13}** led to a significant decrease in cell viability at concentrations of 3.1 µM and higher, **$SrPd_{12}$** only at a concentration of 25 µM, and the other three investigated POPs failed to induce significant cytotoxic effects. After 48 h of treatment, a significant decrease in viability was observed at

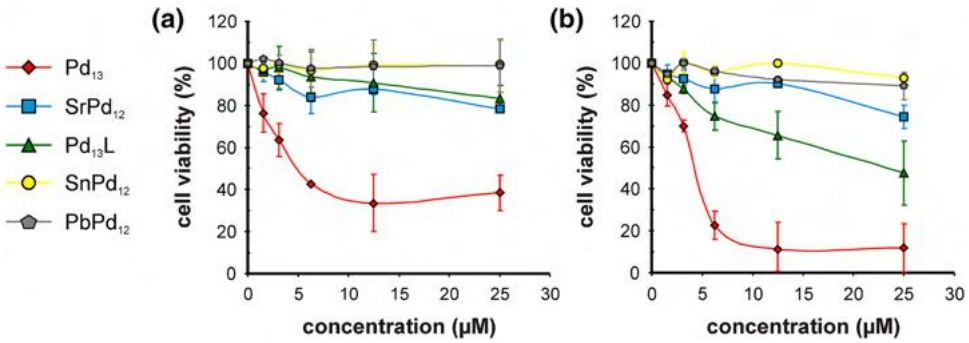

Fig. 2 The effect of POPs on the viability of SH-SY5Y cells. The SH-SY5Y cells were treated with different concentrations of **Pd_{13}**, **$SrPd_{12}$**, **$Pd_{13}L$**, **$SnPd_{12}$** and **$PbPd_{12}$** for 24 h (**a**) and 48 h (**b**), and acid phosphatase assay was performed. The viability of the treated cells was expressed as % of the untreated (control) cells which was arbitrarily set to 100%. The results presented are mean ± S.D. from at least two independent experiments done in triplicates. Asterisks for statistical significance are omitted for clarity

concentrations ≥ 3.1, 6.2, and 12.5 μM for **Pd_{13}**, **$Pd_{13}L$**, and **$SrPd_{12}$**, respectively. On the contrary, neither **$SnPd_{12}$** nor **$PbPd_{12}$** significantly affected the viability of neuroblastoma cells, at both investigated time points. However, both **$SnPd_{12}$** and **$PbPd_{12}$** demonstrated the antileukemic activity [36] suggesting tumor cell specificity in their action.

Calculation of IC_{50} values is presented in detail in supplementary Table S1. Furthermore, Table 1 shows obtained IC_{50} values for the investigated POPs against SH-SY5Y compared to cisplatin, the gold standard among metal-based chemotherapeutics that was used as a positive control. The effect of cisplatin on viability of SH-SY5Y cells (24 and 48 h) is available in supplementary Fig. S1. **Pd_{13}** showed dose-dependent cytotoxic activity and it was the most efficient (lowest IC_{50} value) amongst the investigated POPs, with IC_{50} values lower than cisplatin, at both investigated time points. The obtained IC_{50} value after 48 h treatment for **$Pd_{13}L$** was comparable to cisplatin and significantly lower compared to the 24 h treatment. This indicates that only **$Pd_{13}L$** has time-dependant cytotoxicity, whereas other POPs have not. Although the antitumor activity of POMs has been investigated for many years, reports on human neuroblastoma SH-SY5Y as model system are very scarce. A similar inhibitory action towards SH-SY5Y cell proliferation (IC_{50} of 43 μM) was reported for a POM-based compound constructed from Strandberg-type polyoxometalate diphosphopentamolybdate and benzimidazole [46]. Despite many reports of organically modified POMs with the antitumor potential as well as selectivity higher than corresponding unmodified POMs [26, 27], our results revealed a higher antineuroblastoma potential for pure inorganic POP, **Pd_{13}**, than for two organically modified POPs, **$Pd_{13}L$** and **$SrPd_{12}$**. Considering the fact that two other inorganic POPs, **$SnPd_{12}$** and **$PbPd_{12}$**, regardless of their potent antileukemic action [36], had no significant effect on the viability of SH-SY5Y, it seems that charge (-8) of **Pd_{13}**, might be a dominant factor which is responsible for its highest activity against SH-SY5Y. In addition, regarding the chemical composition, it could be noticed that the satisfactory antineuroblastoma action was induced by arsenic containing POPs (**Pd_{13}**, **$Pd_{13}L$**, and **$SrPd_{12}$**), indicating the need for the comprehensive investigation of their metabolic stability as well as toxicological studies.

Table 1 IC_{50} values of investigated POPs against SH-SY5Y cell line at two time points (24 h and 48 h)

compound	IC_{50} (μM)	
	24 h	48 h
Pd_{13}	7.2 ± 2.2*	4.4 ± 1.2$^{\#}$
$SrPd_{12}$	75.8 ± 6.7	76.7 ± 22.9
$Pd_{13}L$	63.8 ± 3.6	21.4 ± 10.8$^{\#\S}$
$SnPd_{12}$	>> 100	>> 100
$PbPd_{12}$	>> 100	> 100
CDDP	28.4 ± 7.4	11.6 ± 0.8

Values presented are mean ± S.D. from two or three experiments done in triplicate/sextuplicate

CDDP cisplatin

*$p < 0.05$ compared to **$SrPd_{12}$**, **$Pd_{13}L$**, **$SnPd_{12}$** and **$PbPd_{12}$** after 24 h treatment; $^{\#}p < 0.05$ compared to **$SrPd_{12}$**, **$SnPd_{12}$** and **$PbPd_{12}$** after 48 h treatment; $^{\S}p < 0.05$ compared to corresponding 24 h treatment

Investigation of the molecular mechanisms of POP-induced antitumor action

The molecular mechanism of the POP-induced cytotoxic effect was investigated for **Pd_{13}**, **$SrPd_{12}$**, and **$Pd_{13}L$** upon proving their cytotoxic potential against neuroblastoma cells. The concentrations used for these experiments were based on the calculated IC_{50} values for 24 h treatment for each of the POPs.

Oxidative stress and mitochondrial damage induction

Pd_{13} induced ~ 30% increase in the production of the superoxide ion (O_2^-), 4 h after treatment, as determined by an increase in superoxide-specific DHE red fluorescence intensity (Fig. 3a). The superoxide anion radical is usually produced by mitochondria, by one-electron reduction of O_2, and could both be the cause or the consequence of mitochondrial inner membrane dysfunction accompanied by mitochondrial depolarization [47]. However, only 2 h of treatment with **Pd_{13}** caused an increase in JC-1 green-to-red fluorescence ratio (FL1/FL2 = 1.0 for control, FL1/FL2 = 1.46 for **Pd_{13}**), indicative of mitochondrial depolarization (Fig. 3b). These results suggest that **Pd_{13}** first disrupts the mitochondrial membrane function which then leads to an electron leakage and superoxide overproduction. Unlike **Pd_{13}**, both **$SrPd_{12}$** and **$Pd_{13}L$** did not affect the mitochondrial membrane potential and superoxide production after short (2 h and 4 h) exposure (data not shown). Furthermore, similar to **Pd_{13}**, **$SnPd_{12}$** and **$PbPd_{12}$** induced oxidative stress of human leukemic HL-60 cells causing the increase in total production of reactive oxygen species, but unlike **Pd_{13}**, without causing a depolarization of the inner mitochondrial membrane [36].

Apoptosis assessment

The activation of caspases, proteases that elicit and propagate signaling events resulting in cellular death [48], was investigated having in mind their role in different types of regulated cell death [49] and proven oxidative stress and mitochondria involvement in the action of **Pd_{13}**. After 24 h treatment, **Pd_{13}** induced a ~ 30% increase in pancaspase

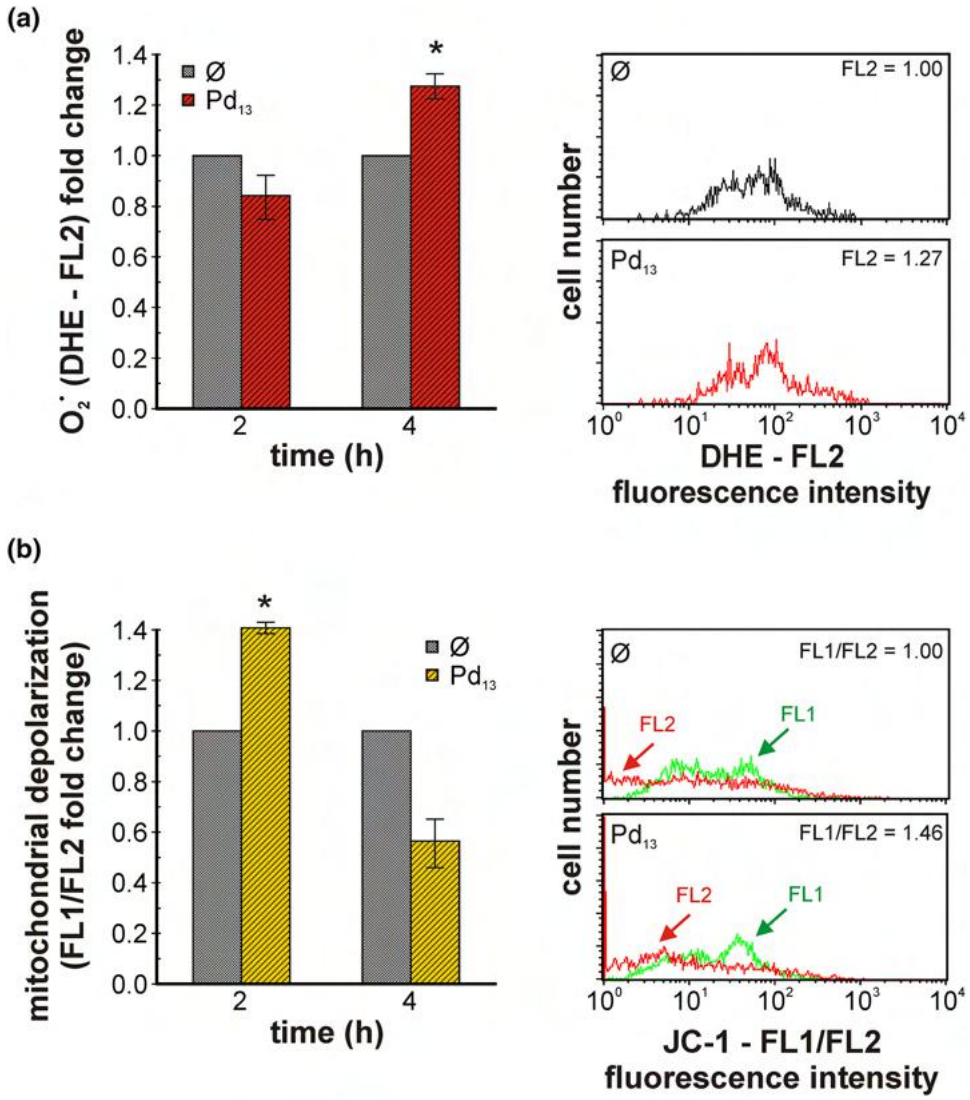

Fig. 3 $\mathbf{Pd_{13}}$ induces superoxide production and mitochondrial depolarization. SH-SY5Y cells were treated with IC_{50} concentration of $\mathbf{Pd_{13}}$ for 2 and 4 h, and the production of superoxide ($O_2^{\cdot}$) (**a**) was assessed using DHE fluorochrome. The results are presented as fold change in red (FL2) median fluorescence intensity in treated cells ± S.D. compared to untreated cells (Ø—set to 1.0) from two independent experiments (left panel) with representative histograms (4 h, right panel). The mitochondrial depolarization (**b**) is presented as fold change in JC-1-derived FL1 (green) to FL2 (red) median fluorescence intensity ratio in treated cells ± S.D. compared to untreated cells (Ø—set to 1.0) from two independent experiments (left panel) with representative histograms (right panel). *$p < 0.05$ compared to untreated cells (Ø)

activation (Fig. 4a). Interestingly, $\mathbf{Pd_{13}L}$ led to a similar result (Fig. 4c), whereas $\mathbf{SrPd_{12}}$ increased the activity of caspases fivefold (Fig. 4b). These results are in agreement with previously reported mechanism of action of $\mathbf{SnPd_{12}}$ and $\mathbf{PbPd_{12}}$ which also caused pancaspase activation in human leukemic cells [36].

Moreover, the analysis of cell cycle distribution showed that a 24 h treatment with $\mathbf{Pd_{13}}$ significantly increased the percentage (14.4%) of neuroblastoma cells with hypodiploid DNA content ($SubG_0$), which is typical of apoptosis, caused a decrease in the percentage of cells in G_1 phase of the cell cycle, and an increase in the number of cells in the S phase, suggestive of cell cycle arrest (Fig. 5a). On the other hand, both $\mathbf{SrPd_{12}}$ and $\mathbf{Pd_{13}L}$ did not induce an increase in the number of cells with hypodiploid DNA content, but both of them displayed the cell cycle arrest: the reduction of neuroblastoma cells in G_0/G_1 phase and the increase in S phase (Fig. 5b and c). This indicates that $\mathbf{Pd_{13}}$, $\mathbf{SrPd_{12}}$, and $\mathbf{Pd_{13}L}$ cause the cell cycle disturbance, preventing the progress of mitosis and resulting in tumor cell death. This finding also suggests that cell cycle arrest together with pancaspase activation, could be common denominators of investigated POPs' antineuroblastoma mechanism of action. Similar to $\mathbf{Pd_{13}}$, both $\mathbf{SnPd_{12}}$ and $\mathbf{PbPd_{12}}$ caused DNA fragmentation typical for apoptosis of leukemic cells [36].

Intracellular acidic vesicle content assessment

The acidic intracellular vesicles content, suggestive of autophagy, was investigated upon staining with pH-sensitive acridine orange dye. While $\mathbf{Pd_{13}}$ increased the orange to green fluorescence ratio for ~ 45% 24 h after treatment (Fig. 6), supporting intracellular acidification, the other two investigated POPs ($\mathbf{SrPd_{12}}$ and $\mathbf{Pd_{13}L}$) failed to induce a similar effect (data not shown).

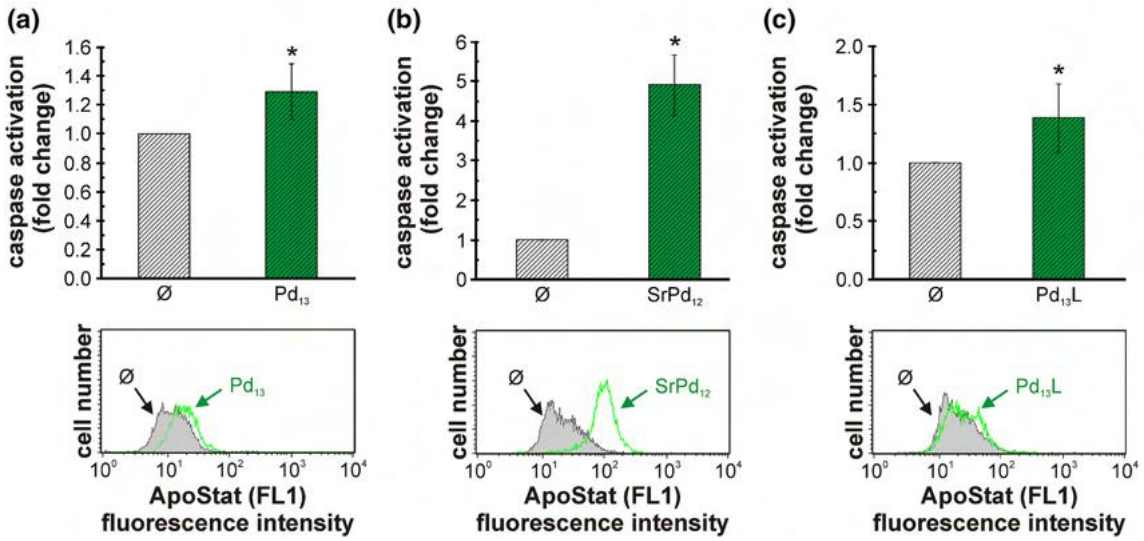

Fig. 4 $\mathbf{Pd_{13}}$, $\mathbf{SrPd_{12}}$ and $\mathbf{Pd_{13}L}$ induce caspase activation. SH-SY5Y cells were treated with IC_{50} concentrations of $\mathbf{Pd_{13}}$ (**a**), $\mathbf{SrPd_{12}}$ (**b**) and $\mathbf{Pd_{13}L}$ (**c**) for 24 h and the caspase activation was determined using FITC-conjugated pancaspase inhibitor ApoStat. The results are presented as fold change in ApoStat-derived green (FL1) median fluorescence intensity ± S.D. in treated cells compared to untreated cells (Ø—set to 1.0) from two independent experiments done in duplicates. Each graph is accompanied by a corresponding representative histogram.*$p < 0.05$ compared to untreated cells (Ø)

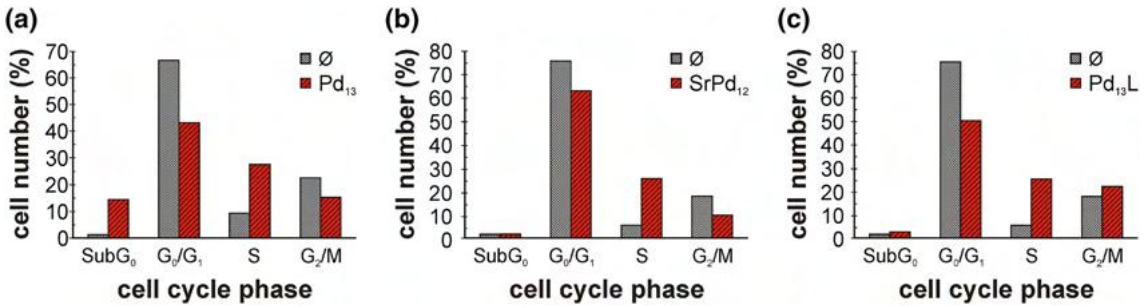

Fig. 5 $\mathbf{Pd_{13}}$, $\mathbf{SrPd_{12}}$ and $\mathbf{Pd_{13}L}$ induce cell cycle arrest. SH-SY5Y cells were treated with IC_{50} concentrations of $\mathbf{Pd_{13}}$ (**a**), $\mathbf{SrPd_{12}}$ (**b**) and $\mathbf{Pd_{13}L}$ (**c**) for 24 h and the percentage of cells in different phases of cell cycle ($SubG_0$, G_0/G_1, S, G_2/M) was assessed using DNA-binding fluorochrome propidium iodide (PI). One of the two independent experiments done in duplicate with similar results is presented

Furthermore, no significant increase in the FL3/FL1 fluorescence ratio was previously detected in HL-60 cells treated with $\mathbf{SnPd_{12}}$ and $\mathbf{PbPd_{12}}$, indicative of an absence of cytoplasmic acidification typical for autophagy [36]. These results suggest that autophagy induction might be a specific mechanism of $\mathbf{Pd_{13}}$ antitumor action. Autophagy involvement in tumor cell death, as a type of antitumor mechanism, was previously reported for some POMs such as the mixed- valence 16-molybdate $[H_2Mo^{V}{}_{12}O_{28}(OH)_{12}(Mo^{VI}O_3)_4]^{6-}$ [50] and the sandwich-type nona-copper(II)-containing 18-tungsto-8-arsenate(III), $[H_4\{Cu^{II}{}_9As^{III}{}_6O_{15}(H_2O)_6\}(\alpha\text{-}As^{III}W_9O_{33})_2]^{8-}$ [51], as well as for some palladium compounds and nanoparticles [18, 52, 53].

Cytogenotoxic effects of POPs on normal cells

Although there are many novel compounds that demonstrate promising results against malignant cells, their potential detrimental effects on physiological processes in non-target healthy cells are the main obstacles for their application as actual therapeutics. Considering this, evaluation of the toxicity towards normal cells is crucial in drug development to find physiologically safe, but yet effective drug candidates. Thus, to assess the toxicological safety using normal human cells, whole blood samples were exposed (for 4 and 24 h) towards the investigated POPs. HPBCs are frequently used as sensitive in vitro models for the toxicity evaluation of cytotoxic chemotherapeutics which affect many types of healthy cells, especially rapidly dividing blood cells [54, 55].

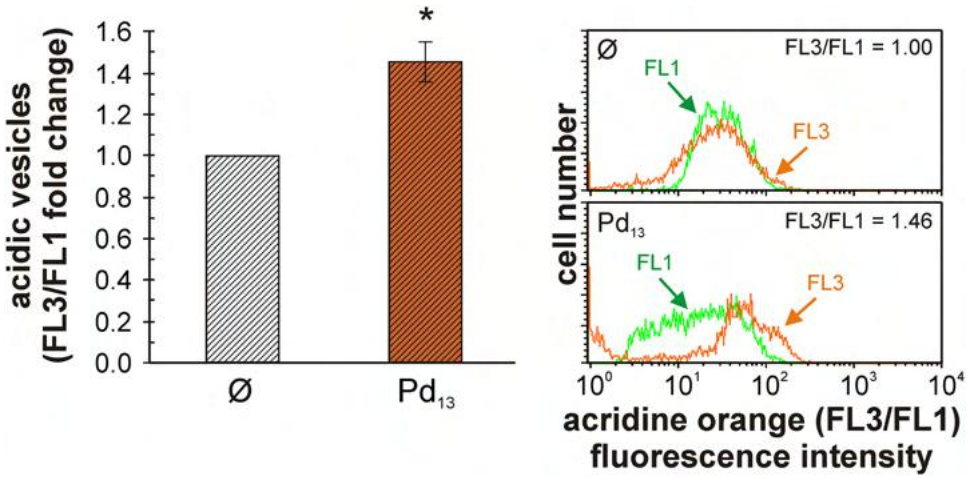

Fig. 6 $\mathbf{Pd_{13}}$ induces an increase of acidic vesicles content in neuroblastoma cells. SH-SY5Y cells were treated with an IC_{50} concentration of $\mathbf{Pd_{13}}$ for 24 h and the number of acidic vesicles was determined by acridine orange staining. The results are presented as fold change in acridine orange-derived FL3 (orange) to FL1 (green) median fluorescence intensity ratio in treated cells ± S.D. compared to untreated control (Ø—set to 1.0) from two independent experiments (left panel) with representative histograms (right panel). *$p < 0.05$ compared to untreated cells (Ø)

For cytogenotoxicity evaluation, three different concentrations of each POP inducing cytotoxic effects on tumor cells (SH-SY5Y for $\mathbf{Pd_{13}}$, $\mathbf{SrPd_{12}}$, and $\mathbf{Pd_{13}L}$, and HL-60 for $\mathbf{SnPd_{12}}$ and $\mathbf{PbPd_{12}}$ [36]) were tested. The effect of the investigated POPs on human PBMC viability is shown in Fig. 7, and the degree of DNA damage, as a genotoxicity indicator, dependent on POP concentrations is presented in Fig. 8.

$\mathbf{Pd_{13}}$, as the most promising antineuroblastoma compound (Table 1; Fig. 2), had no effect on PBMC viabilities even at the highest tested concentration (25 μM ≈ 3 × IC_{50} (24 h) for SH-SY5Y). After both exposure periods to $\mathbf{Pd_{13}}$, the viability of cells was higher than 96%, which was not significantly different from the corresponding controls (Fig. 7a). Moreover, there was no statistically significant difference in the amount of DNA damage, as assessed by the comet assay, in HPBCs compared to the corresponding control samples regardless of the concentration used and exposure time (Fig. 8a). This indicates that $\mathbf{Pd_{13}}$ up to 25 μM is not cytogenotoxic to HPBCs, and therefore $\mathbf{Pd_{13}}$ could be regarded as a promising antineuroblastoma drug candidate with desired selectivity between tumor SH-SY5Y and healthy HPBCs.

Unlike $\mathbf{Pd_{13}}$, the PBMC viability following $\mathbf{SrPd_{12}}$ 24 h exposure was significantly ($p < 0.05$) affected at both 25 and 50 μM (≈ 1/3 and 2/3 IC_{50} (24 h) for SH-SY5Y, respectively) (Fig. 7b). Cell viabilities, expressed as a percentage of the control, of 73.63% ± 8.12 and 58.24% ± 8.98 were obtained for 25 and 50 μM of $\mathbf{SrPd_{12}}$, respectively (Fig. 7b). Furthermore, a significant ($p < 0.05$) increase in primary DNA damage, expressed as a percentage of tail DNA, compared to the corresponding control was noticed after 24 h treatment at the highest concentration tested (50 μM) of $\mathbf{SrPd_{12}}$ (Fig. 8b). Therefore, $\mathbf{SrPd_{12}}$ can be considered toxic towards healthy HPBCs at concentrations ≥ 25 μM.

$\mathbf{Pd_{13}L}$ had no effect on the cell viability and the amount of DNA strand breaks at concentrations ≤ 25 μM (≈ 1/3 IC_{50} (24 h) for SH-SY5Y) regardless of exposure time (Figs. 7c and 8c), whereas a 24 h treatment with 50 μM of $\mathbf{Pd_{13}L}$ (≈ 2/3 IC_{50} (24 h) for SH-SY5Y) induced a significant ($p < 0.05$) decrease in PBMC viability – 64.56% of control (Fig. 7c), as well as a significant ($p < 0.05$) increase in primary DNA damage (Fig. 8c). Thus, $\mathbf{Pd_{13}L}$, applied at concentrations ≤ 25 μM, is regarded as safe to healthy blood cells from a cytogenotoxicity point of view.

No cytotoxicity of $\mathbf{SnPd_{12}}$ and $\mathbf{PbPd_{12}}$, with a demonstrated antileukemic effect against HL-60 [36], was observed on healthy blood cells even at the highest concentration tested (50 μM ≈ 3/2 IC_{50} (24 h) for HL-60). After both exposure periods, the viability of cells was not significantly affected compared to the corresponding controls (Fig. 7d, e). In addition, there was no statistically significant difference in the amount of DNA strand breaks compared to the corresponding control samples for either $\mathbf{SnPd_{12}}$ or $\mathbf{PbPd_{12}}$, regardless of the concentration tested and the exposure time (Fig. 8d, e). Moreover, $\mathbf{SnPd_{12}}$ and $\mathbf{PbPd_{12}}$ demonstrated significant antileukemic activities against HL-60 with similar potencies (IC_{50} (24 h) values of 37.1 ± 4.4 and 34.7 ± 9.2 μM, respectively) [36], and were also inefficient against neuroblastoma cells. Accordingly, in further research, they should be considered as promising, low toxic, and selective antileukemic drug candidates.

The presented results show that $\mathbf{Pd_{13}}$, $\mathbf{SrPd_{12}}$, and $\mathbf{Pd_{13}L}$ are cytotoxic towards human neuroblastoma cells. Amongst them, $\mathbf{Pd_{13}}$ was found to be the most potent with IC_{50} values

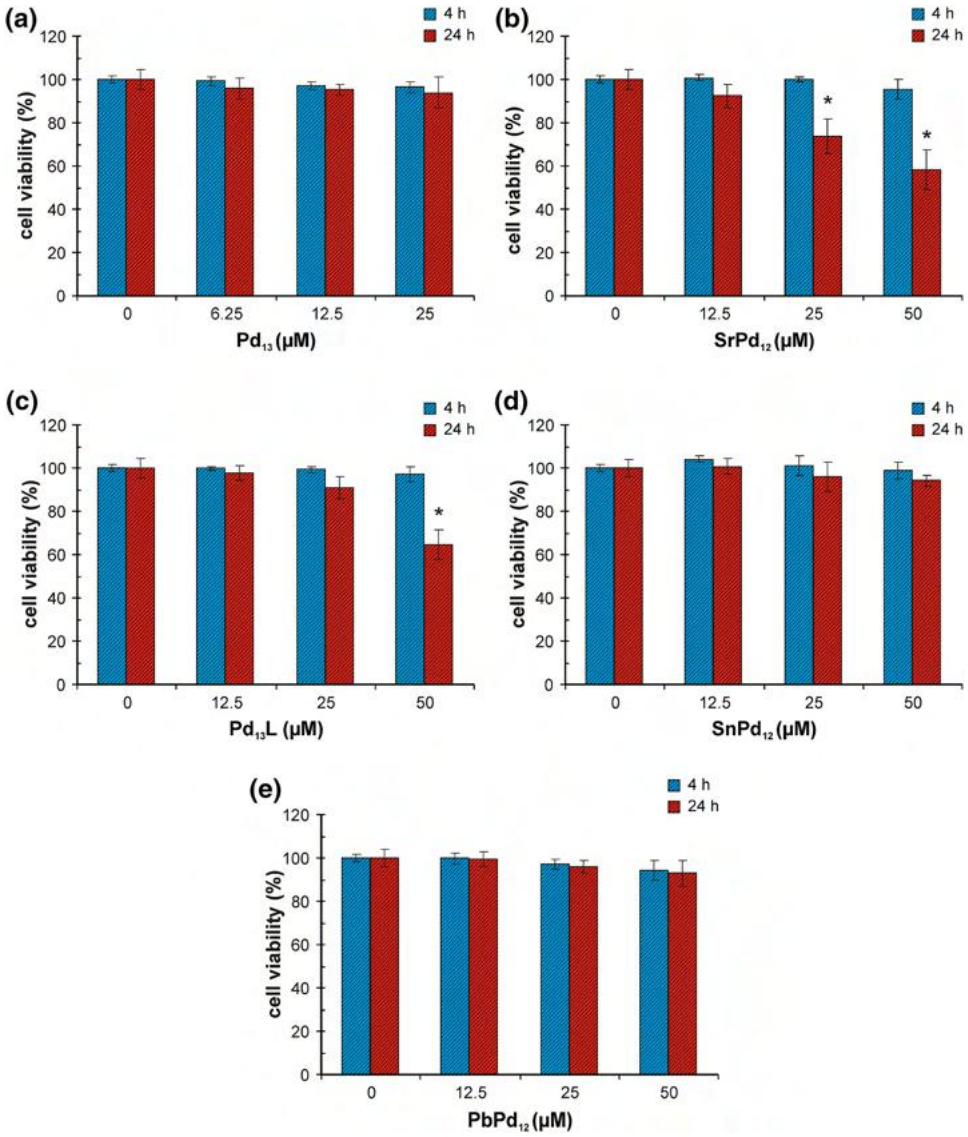

Fig. 7 The effects on the viability in PBMCs after the exposure for 4 and 24h to POPs: $\mathbf{Pd_{13}}$ (**a**), $\mathbf{SrPd_{12}}$ (**b**), $\mathbf{Pd_{13}L}$ (**c**), $\mathbf{SnPd_{12}}$ (**d**), $\mathbf{PbPd_{12}}$ (**e**). The cell viability was determined by differential staining with acridine orange and ethidium bromide after exposure to the POPs for 4 and 24 h. *Statistically significant compared to the corresponding control ($p < 0.05$)

(24 and 48 h) even lower than cisplatin. On the contrary, $\mathbf{SnPd_{12}}$ and $\mathbf{PbPd_{12}}$, despite their promising antileukemic potential [36], do not affect the viability of SH-SY5Y. It can be noticed that pure inorganic POPs, $\mathbf{Pd_{13}}$, $\mathbf{SnPd_{12}}$, and $\mathbf{PbPd_{12}}$, are able to induce DNA fragmentation and oxidative stress in the tumor cells, in contrast to organically modified polyanions, $\mathbf{SrPd_{12}}$ and $\mathbf{Pd_{13}L}$. Besides, only $\mathbf{Pd_{13}}$ causes a depolarization of the inner mitochondrial membrane in SH-SY5Y cells, as well as an increase in acidic vesicles content in cytoplasm, suggestive of autophagy induction. Furthermore, the mechanisms of action of all studied POPs are mediated through pancaspase activation and disturbance of cell cycle in the investigated tumor cells (SH-SY5Y for $\mathbf{Pd_{13}}$, $\mathbf{SrPd_{12}}$, and $\mathbf{Pd_{13}L}$, and HL-60 for $\mathbf{SnPd_{12}}$ and $\mathbf{PbPd_{12}}$ [28]), which is associated with apoptosis. Moreover, the POM-induced activation of the apoptotic pathway as the putative mode of antitumor activity was reported for many classical as well as organically modified POMs [26–28, 50, 56, 57].

The considerable antitumor activities obtained for $\mathbf{Pd_{13}}$, $\mathbf{SrPd_{12}}$, and $\mathbf{Pd_{13}L}$ are comparable with reported antineuroblastoma action of palladium(II) complexes that have been extensively studied as a promising alternative to platinum-based chemotherapeutics [18, 23, 58, 59]. A similar cytotoxicity ($IC_{50} = 26.1 \pm 4.8$ and 2.9 ± 0.2 μM for 24 and 48 h, respectively) against SH-SY5Y cells was published for [PdCl(terpy)](sac)·$2H_2O$ (terpy = 2,2′:6′,2″-terpyridine and sac = saccharinate) [58], and antiproliferative effects of palladium(II) complexes of 5-nitrosopyrimidines on human neuroblastoma NB69 cell line were recorded within the concentration range 2–10 μM [59]. Accordingly, the presented results indicate that the investigation of POP antitumor properties is a promising research direction in the development of next-generation antitumor metallodrugs.

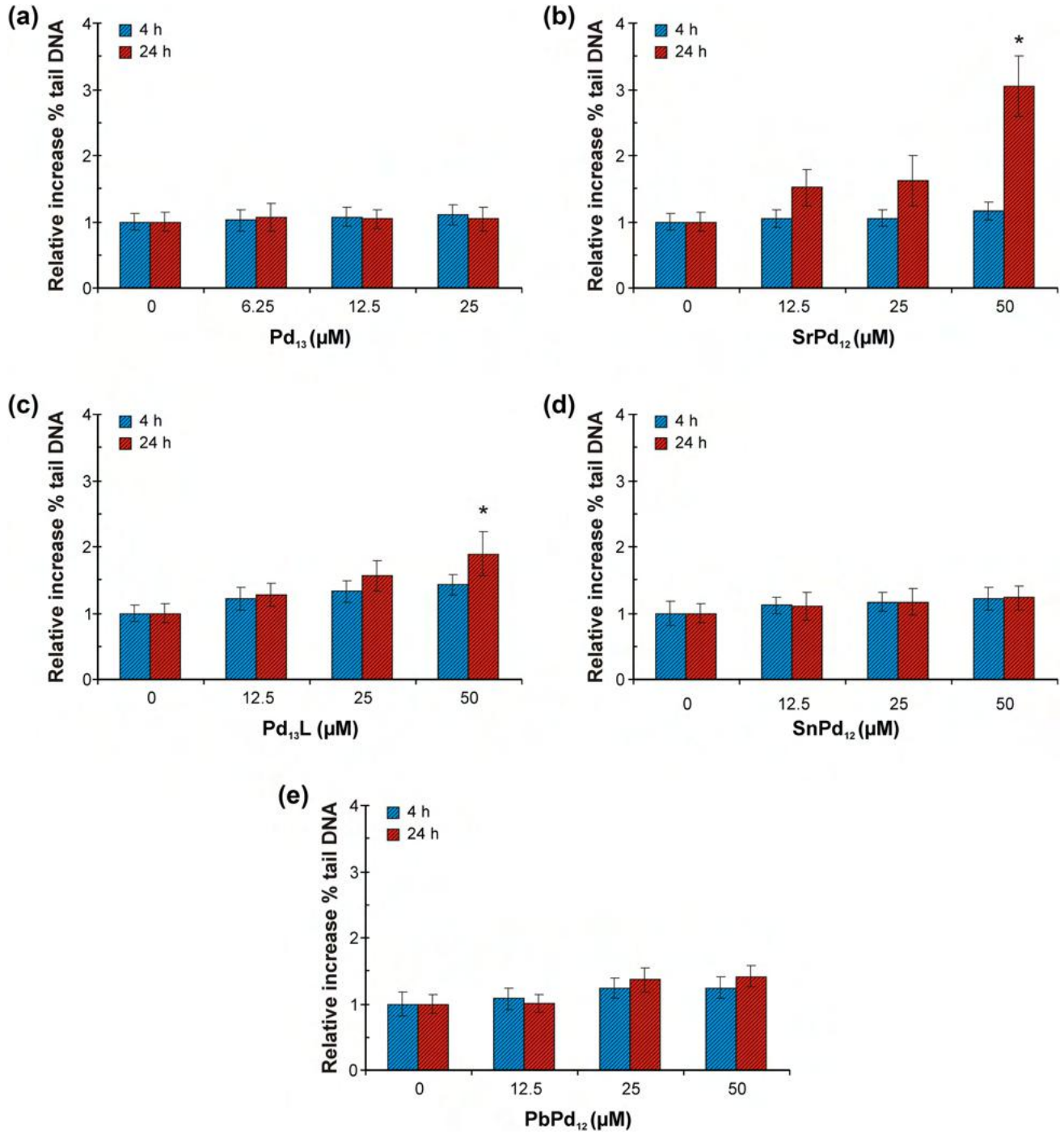

Fig. 8 The effects on DNA damage in HPBCs after the exposure for 4 and 24 h to POPs $\mathbf{Pd_{13}}$ (**a**), $\mathbf{SrPd_{12}}$ (**b**), $\mathbf{Pd_{13L}}$ (**c**), $\mathbf{SnPd_{12}}$ (**d**), $\mathbf{PbPd_{12}}$ (**e**). The DNA damage was assessed with the alkaline comet assay after exposure to the POPs for 4 and 24 h and is expressed as % of tail DNA. * Statistically significant compared to the corresponding control ($p < 0.05$)

Interestingly, the obtained results revealed that inorganic nanocubic POPs, $\mathbf{Pd_{13}}$, $\mathbf{SnPd_{12}}$, and $\mathbf{PbPd_{12}}$, did not show cytogenotoxicity against normal non-target blood cells at the concentrations inducing considerable antitumor effects. The obtained prominent selectivity between tumor and normal HPBCs clearly identifies $\mathbf{Pd_{13}}$, $\mathbf{SnPd_{12}}$ and $\mathbf{PbPd_{12}}$ as promising antitumor drug candidates, keeping in mind that side effects of potential therapeutics are well known as a major limitation in their clinical application. Furthermore, it is worthy to note that $\mathbf{Pd_{13}}$, despite the arsenic content, does not act cytogenotoxic to the healthy blood cells even at 25 μM (Figs. 7a and 8a) inducing

the remarkable decrease (≈ 60%) in SH-SY5Y viability (Fig. 2a). This observation might be assigned to a good metabolic stability of $\mathbf{Pd_{13}}$ under the employed experimental conditions. On the other hand, the other investigated arsenic containing POPs, $\mathbf{SrPd_{12}}$, and $\mathbf{Pd_{13}L}$, caused cytogenotoxic action to the healthy cells after 24 h treatment (Figs. 7b,c and 8b,c) at antineuroblastoma inducing concentrations (≈ IC_{50} (24 h) for SH-SY5Y), which points out a necessity of performing extensive mechanistic studies. Despite the importance of relevant toxicity data, many studies on palladium compounds with effective antitumor activity lack an assessment of their impact on healthy cells. Moreover, some Pd(II) complexes of 3,5-dimethyl-1-thiocarbamoylpyrazole were reported as having even greater toxicity than cisplatin against healthy cells [60], which underlines the importance of our study.

Conclusions

In summary, $\mathbf{Pd_{13}}$ can be regarded as the most promising antineuroblastoma agent among all investigated POPs. It demonstrated the lowest IC_{50} value, even lower than cisplatin for both 24 and 48 h time points, but yet without statistically confirmed time dependence supportive of its effectiveness. Furthermore, $\mathbf{Pd_{13}}$ caused mitochondrial membrane depolarisation prior to superoxide ion hyperproduction, followed with caspase activation, DNA fragmentation and cell cycle arrest, all hallmarks of apoptotic cell death, and accompanied with the increase in acidic vesicles content suggestive of autophagy induction. Moreover, $\mathbf{Pd_{13}}$ demonstrated the desired pharmacological response at concentrations not injurious to the structural and functional integrity of the healthy non-target HPBCs. In addition, the results of this study confirmed both $\mathbf{SnPd_{12}}$ and $\mathbf{PbPd_{12}}$ as promising antileukemic drug candidates showing tumor cell specificity and good selectivity.

Supplementary Information The online version contains supplementary material available at https://doi.org/10.1007/s00775-021-01905-4.

Acknowledgements This study received funding from the Ministry of Education, Science and Technological Development, Republic of Serbia (grant agreements no. 451-03-9/2021-14/200110 and 451-03-9/2021-14/200017), the Institute for Medical Research and Occupational Health, Zagreb, Croatia, the German Research Council (DFG, KO-2288/20-1) and Jacobs University. The authors also gratefully acknowledge the bilateral projects: Serbia-Germany (no. 451-03-01038/2015-09/16, DAAD-PPP) and Serbia-Croatia (no. 337-00-205/2019-09/19), and COST Actions: CMST CM1203—PoCheMoN, CA16113 – CliniMARK, and CA15132 – hCOMET. MČ and DK would like to thank COST Action CA16113 – CliniMARK for supporting this research with Short-Term Scientific Mission (STSM 44119 and 44120). Figure 1 is generated with Diamond, version 3.2 (Crystal Impact GbR).

Declarations

Conflict of interest The authors have no conflicts of interest to declare that are relevant to the content of this article.

Consent for publication All authors agreed with the content of the paper and gave consent for submission and publication.

References

1. Williams CJ, Whitehouse JMA (1979) Cisplatinum: a new anticancer agent. Br Med J 1:1689–1691
2. Momić TG, Čolović MB, Lazarević-Pašti TD, Vasić VM (2016) Metal based compounds, modulators of Na, K-ATPase with anticancer activity. In: Chakraborti S, Dhalla NS (eds) Advances in biochemistry in health and disease, regulation of membrane Na^+-K^+-ATPase. Springer International Publishing, Berlin. https://doi.org/10.1007/978-3-319-24750-224
3. Fanelli M, Formica M, Fusi V, Giorgi L, Micheloni M, Paoli P (2016) New trends in platinum and palladium complexes as antineoplastic agents. Coord Chem Rev 310:41–79. https://doi.org/10.1016/j.ccr.2015.11.004
4. Deo KM, Ang DL, McGhie B, Rajamanickam A, Dhiman A, Khoury A, Holland J, Bjelosevic A, Pages B, Gordon C, Aldrich-Wright JR (2018) Platinum coordination compounds with potent anticancer activity. Coord Chem Rev 375:148–163. https://doi.org/10.1016/j.ccr.2017.11.014
5. Brabec V, Hrabina O, Kasparkova J (2017) Cytotoxic platinum coordination compounds. DNA binding agents. Coord Chem Rev 351:2–31. https://doi.org/10.1016/j.ccr.2017.04.013
6. Farrell NP (2015) Multi-platinum anti-cancer agents. Substitution-inert compounds for tumor selectivity and new targets. Chem Soc Rev 44(24):8773–8785. https://doi.org/10.1039/c5cs00201j
7. Khoury A, Deo KM, Aldrich-Wright JR (2020) Recent advances in platinum-based chemotherapeutics that exhibit inhibitory and targeted mechanisms of action. J Inorg Biochem 207:111070. https://doi.org/10.1016/j.jinorgbio.2020.111070
8. Yao X, Panichpisal K, Kurtzman N, Nugent K (2007) Cisplatin nephrotoxicity: a review. Am J Med Sci 334(2):115–124. https://doi.org/10.1097/maj.0b013e31812dfe1e
9. Niioka T, Uno T, Yasui-Furukori N, Takahata T, Shimizu M, Sugawara K, Tateishi T (2007) Pharmacokinetics of low-dose nedaplatin and validation of AUC prediction in patients with non-small-cell lung carcinoma. Cancer Chemother Pharmacol 59:575–580. https://doi.org/10.1007/s00280-006-0298-2
10. Hartmann JT, Lipp H-P (2003) Toxicity of platinum compounds. Expert Opin Pharmacother 4(6):889–901. https://doi.org/10.1517/14656566.4.6.889
11. Rottenberg S, Disler C, Perego P (2021) The rediscovery of platinum-based cancer therapy. Nat Rev Cancer 21(1):37–50. https://doi.org/10.1038/s41568-020-00308-y
12. Zahreddine H, Borden KLB (2013) Mechanisms and insights into drug resistance in cancer. Front Pharmacol. https://doi.org/10.3389/fphar.2013.00028
13. Johnstone TC, Suntharalingam K, Lippard SJ (2016) The next generation of platinum drugs: targeted Pt(II) agents, nanoparticle delivery, and Pt(IV) prodrugs. Chem Rev 116(5):3436–3486. https://doi.org/10.1021/acs.chemrev.5b00597
14. Omondi RO, Ojwach SO, Jaganyi D (2020) Review of comparative studies of cytotoxic activities of Pt(II), Pd(II), Ru(II)/(III) and Au(III) complexes, their kinetics of ligand substitution reactions and DNA/BSA interactions. Inorg Chim Acta 512:119883. https://doi.org/10.1016/j.ica.2020.119883

15. Gill DS (1984) Structure activity relationship of antitumor palladium complexes. In: Hacker MP, Douple EB, Krakoff IH (eds) Platinum coordination complexes in cancer chemotherapy. Developments in oncology. Springer, Boston. https://doi.org/10.1007/978-1-4613-2837-7_21
16. Puthraya KH, Srivastava TS, Amonkar AJ, Adwankar MK, Chitnis MP (1986) Some potential anticancer palladium(II) complexes of 2,2'-bipyridine and amino acids. J Inorg Biochem 26(1):45–54. https://doi.org/10.1016/0162-0134(86)80035-6
17. Mital R, Jain N, Srivastava TS (1989) Synthesis, characterization and cytotoxic studies of diamine and diimine palladium(II) complexes of diethyldithiocarbamate and binding of these and analogous platinum(II) complexes with DNA. Inorg Chim Acta 166(1):135–140. https://doi.org/10.1016/s0020-1693(00)80798-7
18. Alam MN, Huq F (2016) Comprehensive review on tumour active palladium compounds and structure–activity relationships. Coord Chem Rev 316:36–67. https://doi.org/10.1016/j.ccr.2016.02.001
19. Vojtek M, Marques MPM, Ferreira IMPLVO, Mota-Filipe H, Diniz C (2019) Anticancer activity of palladium-based complexes against triple-negative breast cancer. Drug Discov Today 24(4):1044–1058. https://doi.org/10.1016/j.drudis.2019.02.012
20. de Souza RFF, da Cunha GA, Pereira JCM, Garcia DM, Bincoletto C, Goto RN, Leopoldino AM, da Silva IC, Pavan FR, Deflon VM, de Almeida ET, Mauro AE, Netto AV (2019) Orthopalladated acetophenone oxime compounds bearing thioamides as ligands: synthesis, structure and cytotoxic evaluation. Inorg Chim Acta 486:617–624. https://doi.org/10.1016/j.ica.2018.11.022
21. Štarha P, Trávníček Z (2019) Non-platinum complexes containing releasable biologically active ligands. Coord Chem Rev 395:130–145. https://doi.org/10.1016/j.ccr.2019.06.001
22. Misirlic-Dencic S, Poljarevic J, Isakovic AM, Sabo T, Markovic I, Trajkovic V (2020) Current development of metal complexes with diamine ligands as potential anticancer agents. Curr Med Chem 27(3):380–410. https://doi.org/10.2174/0929867325666181031114306
23. Carneiro TJ, Martins AS, Marques MPM, Gil AM (2020) Metabolic aspects of palladium(II) potential anti-cancer drugs. Front Oncol 10:590970. https://doi.org/10.3389/fonc.2020.590970
24. Yanagie H, Ogata A, Mitsui S, Hisa T, Yamase T, Eriguchi M (2006) Anticancer activity of polyoxomolybdate. Biomed Pharmacother 60:349–352. https://doi.org/10.1016/j.biopha.2006.06.018
25. Yamase T (2013) Polyoxometalates active against tumors, viruses, and bacteria. Prog Mol Subcell Biol 54:65–116. https://doi.org/10.1007/978-3-642-41004-8_4
26. Bijelic A, Aureliano M, Rompel A (2019) Polyoxometalates as potential next-generation metallodrugs in the combat against cancer. Angew Chem Int Ed 58:2980–2999. https://doi.org/10.1002/anie.201803868
27. Čolović MB, Lacković M, Lalatović J, Mougharbel AS, Kortz U, Krstić DZ (2020) Polyoxometalates in biomedicine: update and overview. Curr Med Chem 27:362–379. https://doi.org/10.2174/0929867326666190827153532
28. Yamase T (2005) Anti-tumor, -viral, and -bacterial activities of polyoxometalates for realizing an inorganic drug. J Mater Chem 15:4773–4782. https://doi.org/10.1039/B504585A
29. Aureliano M, Gumerova NI, Sciortino G, Garribba E, Rompel A, Crans DC (2021) Polyoxovanadates with emerging biomedical activities. Coord Chem Rev 447:214143. https://doi.org/10.1016/j.ccr.2021.214143
30. Lu F, Wang M, Li N, Tang B (2021) Polyoxometalate-based nanomaterials toward efficient cancer diagnosis and therapy. Chemistry 27(21):6422–6434. https://doi.org/10.1002/chem.202004500
31. Izarova NV, Pope MT, Kortz U (2012) Noble metals in polyoxometalates. Angew Chem Int Ed 51(38):9492–9510. https://doi.org/10.1002/anie.201202750
32. Yang P, Kortz U (2018) Discovery and evolution of polyoxopalladates. Acc Chem Res 51(7):1599–1608. https://doi.org/10.1021/acs.accounts.8b00082
33. Chubarova EV, Dickman MH, Keita B, Nadjo L, Miserque F, Mifsud M, Arends IWCE, Kortz U (2008) Self-Assembly of a heteropolyoxopalladate nanocube: $[Pd^{II}_{13}AsV_8O_{34}(OH)_6]^{8-}$. Angew Chem Int Ed 47(49):9542–9546. https://doi.org/10.1002/anie.200803527
34. Yang P, Xiang Y, Lin Z, Bassil BS, Cao J, Fan L, Fan Y, Li M-X, Jiménez-Lozano P, Carbó JJ, Poblet JM, Kortz U (2014) Alkaline earth guests in polyoxopalladate chemistry: from nanocube to nanostar via an open-shell structure. Angew Chem Int Ed 53(44):11974–11978. https://doi.org/10.1002/anie.201407090
35. Izarova NV, Dickman MH, Biboum RN, Keita B, Nadjo L, Ramachandran V, Dalal NS, Kortz U (2009) Heteropoly-13-palladates(II) $[Pd^{II}_{13}(As^{V}Ph)_8O_{32}]^{6-}$ and $[Pd^{II}_{13}Se^{IV}_8O_{32}]^{6-}$. Inorg Chem 48(16):7504–7506. https://doi.org/10.1021/ic900953a
36. Yang P, Ma T, Lang Z, Misirlic-Dencic S, Isakovic AM, Bényei A, Čolović MB, Markovic I, Krstić DZ, Poblet JM, Lin Z, Kortz U (2019) Tetravalent metal ion guests in polyoxopalladate chemistry: synthesis and anticancer activity of $[MO_8Pd_{12}(PO_4)_8]^{12-}$ ($M = Sn^{IV}$, Pb^{IV}). Inorg Chem 58(17):11294–11299. https://doi.org/10.1021/acs.inorgchem.9b01129
37. Aravindan N, Herman T, Aravindan S (2020) Emerging therapeutic targets for neuroblastoma. Expert Opin Ther Targets 24(9):899–914. https://doi.org/10.1080/14728222.2020.1790528
38. Hua Y, Zhou N, Zhang J, Zhang Z, Li N, Wang J, Zheng W, Li X, Wang F, Zhang L, Hou L (2020) Isatin inhibits the invasion and metastasis of SH-SY5Y neuroblastoma cells in vitro and in vivo. Int J Oncol 58(1):122–132. https://doi.org/10.3892/ijo.2020.5144
39. Misirlić Denčić S, Poljarević J, Isakovic AM, Marković I, Sabo TJ, Grgurić-Šipka S (2017) Antileukemic action of novel diamine Pt(II) halogenido complexes: comparison of the representative novel Pt(II) with corresponding Pt(IV) complex. Chem Biol Drug Des 90(2):262–271. https://doi.org/10.1111/cbdd.12945
40. Savić A, Misirlić-Denčić S, Dulović M, Mihajlović-Lalić LE, Jovanović M, Grgurić-Šipka S, Marković I, Sabo TJ (2014) Synthesis, characterization and ROS-mediated cytotoxic action of novel (S, S)-1,3-propanediamine-N, N′-di-2-(3-cyclohexyl)propanoic acid and corresponding esters. Bioorg Chem 54:73–80. https://doi.org/10.1016/j.bioorg.2014.04.006
41. Raicevic N, Mladenovic A, Perovic M, Harhaji L, Miljkovic D, Trajkovic V (2005) Iron protects astrocytes from 6-hydroxydopamine toxicity. Neuropharmacology 48(5):720–731. https://doi.org/10.1016/j.neuropharm.2004.12.003
42. Atale N, Gupta S, Yadav U, Rani V (2014) Cell-death assessment by fluorescent and nonfluorescent cytosolic and nuclear staining techniques. Microsc-JPN 255(1):7–19. https://doi.org/10.1111/jmi.12133
43. Singh NP, McCoy MT, Tice RR, Schneider EL (1988) A simple technique for quantitation of low levels of DNA damage in individual cells. Exp Cell Res 175(1):184–191. https://doi.org/10.1016/0014-4827(88)90265-0
44. Gajski G, Garaj-Vrhovac V, Oreščanin V (2008) Cytogenetic status and oxidative DNA-damage induced by atorvastatin in human peripheral blood lymphocytes: standard and Fpg-modified comet assay. Toxicol Appl Pharm 231(1):85–93. https://doi.org/10.1016/j.taap.2008.03.013
45. Møller P, Azqueta A, Boutet-Robinet E, Koppen G, Bonassi S, Milić M, Gajski G, Costa S, Teixeira JP, Costa Pereira C, Dusinska M, Godschalk R, Brunborg G, Gutzkow KB, Giovannelli L, Cooke MS, Richling E, Laffon B, Valdiglesias V, Langie SAS (2020) Minimum Information for Reporting on the Comet Assay (MIRCA): recommendations for describing comet assay

procedures and results. Nat Protoc 15(12):3817–3826. https://doi.org/10.1038/s41596-020-0398-1
46. Qu X, Feng H, Ma C, Yang Y, Yu X (2017) Synthesis, crystal structure and anti-tumor activity of a novel 3D supramolecular compound constructed from Strandberg-type polyoxometalate and benzimidazole. Inorg Chem Commun 81:22–26. https://doi.org/10.1016/j.inoche.2017.04.023
47. Sinha K, Das J, Pal PB, Sil PC (2013) Oxidative stress: the mitochondria-dependent and mitochondria-independent pathways of apoptosis. Arch Toxicol 87(7):1157–1180. https://doi.org/10.1007/s00204-013-1034-4
48. Ramirez MLG, Salvesen GS (2018) A primer on caspase mechanisms. Semin Cell Dev Biol 82:79–85. https://doi.org/10.1016/j.semcdb.2018.01.002
49. Abate M, Festa A, Falco M, Lombardi A, Luce A, Grimaldi A, Zappavigna S, Sperlongano P, Irace C, Caraglia M, Misso G (2020) Mitochondria as playmakers of apoptosis, autophagy and senescence. Semin Cell Dev Biol 98:139–153. https://doi.org/10.1016/j.semcdb.2019.05.022
50. Ogata A, Yanagie H, Ishikawa E, Morishita Y, Mitsui S, Yamashita A, Hasumi K, Takamoto S, Yamase T, Eriguchi M (2008) Antitumour effect of polyoxomolybdates: induction of apoptotic cell death and autophagy in in vitro and in vivo models. Br J Cancer 98:399–409. https://doi.org/10.1038/sj.bjc.6604133
51. Zhou Z, Zhang D, Yang L, Ma P, Si Y, Kortz U, Niu J, Wang J (2013) Nona-copper(II)-containing 18-tungsto-8-arsenate(III) exhibits antitumor activity. Chem Commun 49:5189–5191. https://doi.org/10.1039/c3cc41628c
52. Alqatati A, Hamad Elgazwy A-SS, Aliwaini S (2020) Newly synthesized palladium (II) complex ASH10 induces apoptosis and autophagy in breast cancer cells. Int J Cancer Res 16(2):40–47. https://doi.org/10.3923/ijcr.2020.40.47
53. Zhang L, Chen X, Wu J, Ding S, Wang X, Lei Q, Fang W (2018) Palladium nanoparticles induce autophagy and autophagic flux blockade in Hela cells. RSC Adv 8(8):4130–4141. https://doi.org/10.1039/c7ra11400a
54. Sakai H, Kokura S, Ishikawa T, Tsuchiya R, Okajima M, Matsuyama T, Adachi S, Katada K, Kamada K, Uchiyama K, Handa O, Takagi T, Yagi N, Naito Y, Yoshikawa T (2013) Effects of anticancer agents on cell viability, proliferative activity and cytokine production of peripheral blood mononuclear cells. J Clin Biochem Nutr 52(1):64–71. https://doi.org/10.3164/jcbn.12-60
55. Smrečki N, Rončević T, Jović O, Kukovec BM, Maravić A, Gajski G, Čikeš-Čulić V (2019) Copper(II) complexes with N′-methylsarcosinamide selective for human bladder cancer cells. Inorg Chim Acta 488:312–320. https://doi.org/10.1016/j.ica.2019.01.013
56. Zhang Z-M, Duan X, Yao S, Wang Z, Lin Z, Li Y-G, Long L-S, Wang E-B, Lin W (2016) Cation-mediated optical resolution and anticancer activity of chiral polyoxometalates built from entirely achiral building blocks. Chem Sci 7:4220–4229. https://doi.org/10.1039/C5SC04408A
57. Ogata A, Mitsui S, Yanagie H, Kasano H, Hisa T, Yamase T, Eriguchi M (2005) Novel anti-tumor agent, polyoxomolybdate induces apoptotic cell death in AsPC-1 human pancreatic cancer cells. Biomed Pharmacother 59:240–244. https://doi.org/10.1016/j.biopha.2004.11.008
58. Kacar O, Adiguzel Z, Yilmaz VT, Cetin Y, Cevatemre B, Arda N, Baykal AT, Ulukaya E, Acilan C (2014) Evaluation of the molecular mechanisms of a palladium(II) saccharinate complex with terpyridine as an anticancer agent. Anti-cancer Drug 25(1):17–29. https://doi.org/10.1097/CAD.0b013e328364c6ad
59. Illán-Cabeza NA, García-García AR, Martínez-Martos JM, Ramírez-Expósito MJ, Moreno-Carretero MN (2013) Antiproliferative effects of palladium(II) complexes of 5-nitrosopyrimidines and interactions with the proteolytic regulatory enzymes of the renin–angiotensin system in tumoral brain cells. J Inorg Biochem 126:118–127. https://doi.org/10.1016/j.jinorgbio.2013.06.005
60. Rocha FV, Barra CV, Netto AV, Mauro AE, Carlos IZ, Frem RC, Ananias SR, Quilles MB, Stevanato A, da Rocha MC (2010) 3,5-Dimethyl-1-thiocarbamoylpyrazole and its Pd(II) complexes: synthesis, spectral studies and antitumor activity. Eur J Med Chem 45(5):1698–1702. https://doi.org/10.1016/j.ejmech.2009.12.073